Metabolomics (2019) 15:52
https://doi.org/10.1007/s11306-019-1514-5

ORIGINAL ARTICLE

UPLC-MS-based metabolomics reveals metabolic dysregulation in ALDH1A1-overexpressed lung adenocarcinoma cells

Yang Wang[1] · Cong-Hui Wang[1] · Yu-Fei Zhang[1] · Liang Zhu[1] · Hui-Min Lei[1] · Ya-Bin Tang[1]

Received: 8 November 2018 / Accepted: 18 March 2019 / Published online: 25 March 2019

Abstract

Introduction Specific oncogenotypes can produce distinct metabolic changes in cancer. Recently it is considered that metabolic reprograming contributes heavily to drug resistance. Aldehyde dehydrogenase 1A1 (ALDH1A1), is overexpressed in drug resistant lung adenocarcinomas and may be the cause of acquired drug resistance. However, how ALDH1A1 affects metabolic profiling in lung adenocarcinoma cells remains elusive.

Objective We sought to investigate metabolic alterations induced by ALDH1A1 in lung adenocarcinoma in order to better understand the reprogramming and metabolic mechanism of resistance induced by ALDH1A1.

Methods Metabolic alterations in lung adenocarcinoma HCC827-ALDH1A1 cells were analyzed by ultra-performance liquid chromatography-quadrupole time-of-flight mass spectrometry (UPLC–QTOF-MS). HCC827-ALDH1A1 metabolic signatures were extracted by univariate and multivariate statistical analysis. Furthermore, metabolite enrichment analysis and pathway analysis were performed using MetaboAnalyst 4.0 software.

Results Twenty-two metabolites were positively identified using authentic standards, including uridine monophosphate (UMP), uridine diphosphate (UDP), adenosine diphosphate (ADP), malic acid, malonyl-coenzyme A, nicotinamide adenine dinucleotide (NAD), coenzyme A and so on. Furthermore, metabolic pathway analysis revealed several dysregulated pathways in HCC827-ALDH1A1 cells, including nucleotide metabolism, urea cycle, tricarboxylic acid (TCA) cycle, and glycerol phospholipid metabolism etc.

Conclusion Lung cancer is the most frequent cause of cancer-related deaths worldwide. Nearly all patients eventually undergo disease progression due to acquired resistance. Mechanisms of biological acquired resistance need to be identified. Our study identified altered metabolites in HCC827-ALDH1A1 cells, enhancing our knowledge of lung adenocarcinoma metabolic alterations induced by ALDH1A1, creating a novel therapeutic pathway. These metabolic signatures of ALDH1A1 overexpression may shed light on molecular mechanisms in drug-resistant tumors, and on candidate drug targets. Furthermore, new molecular targets may provide the foundation for potential anticancer strategies for lung cancer therapy.

Keywords ALDH1A1 · Tumor resistance · Lung adenocarcinoma · UPLC–QTOF-MS · Cell metabolic profiling

Electronic supplementary material The online version of this article (https://doi.org/10.1007/s11306-019-1514-5) contains supplementary material, which is available to authorized users.

✉ Yang Wang
18817275718@163.com

Cong-Hui Wang
evacino@163.com

Yu-Fei Zhang
Zyflyy@outlook.com

Liang Zhu
zhuliang17@126.com

Hui-Min Lei
leihuimin02@163.com

Ya-Bin Tang
leonyabin2018@shsmu.edu.cn

[1] Department of Pharmacology and Chemical Biology, Shanghai Jiao Tong University School of Medicine, Shanghai 200025, China

1 Introduction

Aldehyde dehydrogenase (ALDH), an enzyme that degrades acetaldehyde, is a characteristic of cancer stem cells (CSC). Nineteen ALDH genes, including ALDH1A1, have been identified in the human genome to form the ALDH superfamily (Vasiliou et al. 2004). The ALDH superfamily is composed of NAD $(P)^+$ dependent enzymes that catalyze the oxidation of aldehydes to non-toxic carboxylic acids (Ueshima et al. 1993; Vasiliou et al. 2000). They catalyze the oxidation of a variety of aldehyde substrates against toxic species in cells. Manzer et al. proposed ALDH1A1 effectively degrades lipid peroxidation derived aldehydes, including 4-HNE and MDA, to eliminate oxidative stress, including ageing and UV radiation (Lassen et al. 2007; Manzer et al. 2003). As a metabolic enzyme, ALDH1A1 plays a key role in cellular defenses against toxic metabolites (Fig. S1).

In addition to degrading acetaldehyde, ALDH activity is also associated with drug resistance (Januchowski et al. 2016; Prabavathy et al. 2018; Tanei et al. 2009). The expression of ALDH enzymes is found to increase in drug-resistant cells, in contrast to drug-sensitive cells (Januchowski et al. 2013; Luo et al. 2012; Wang et al. 2018a). Analogously, lung cancer cells that are resistant to EGFR tyrosine kinase inhibitor (EGFR-TKI), or to chemotherapeutic drugs have higher expression levels of ALDH1A1 (Huang et al. 2013). Lung cancer is the leading cause of cancer-related death in the world today. Globally, approximately 1.6 million new cases are reported each year, and the 5 year survival rate is only 16.6% (Domingues et al. 2014; Siegel et al. 2014; Sundar et al. 2014). Unfortunately, drug resistance is almost inevitable in lung cancer patients, leading to tumor recurrence and poor prognosis after using targeted drugs over a period of time (Kobayashi et al. 2005; Roengvoraphoj et al. 2013). ALDH promotes acquired resistance by metabolizing the chemotherapeutic drug cyclophosphamide, and detoxifying the intermediate product aldophosphamide to a non-toxic carboxyphosphoramide (Bozorgi et al. 2015; Magni et al. 1996). Although ALDH1A1 can induce drug resistance, changes in metabolic networks induced by ALDH1A1 are unclear, and whether the metabolome leads to drug resistance remains uncertain.

The metabolome is a collection of small biochemically active molecules, namely metabolites, with a high level of chemical diversity in biological systems (Nicholson and Lindon 2008). Untargeted metabolomics are global in scope and aim to simultaneously measure as many metabolites (metabolome) as possible from biological samples without bias, which is an important comparative tool to study global metabolite levels in samples under various conditions. Approaches that accelerate measurement of metabolite levels directly from samples shed light on our understanding of the diverse roles of metabolites, and potentially lead to discovery of new and noncommittal mechanisms of drug resistance. Genomics and transcriptomics provide a blueprint for the metabolic activity of organisms. Proteomics is the executor of this blueprint, and metabolomics, reflects real-time changes in the metabolism of organisms, and their phenotypic characteristics. This is the advantage of metabolomics, compared to other approaches (Wettersten 2013). Although untargeted metabolomics can be performed using either NMR or mass spectrometry (MS), MS enables the detection of most metabolites and has, therefore, been the technique of choice for metabolic profiling efforts. Most metabolic profiling studies are currently performed using quadrupole-time-of-flight (QTOF)-MS due to high resolution, sensitivity, rapid data acquisition, and high mass accuracy. The development of ultra-performance liquid chromatography (UPLC) has made it possible to achieve even higher resolution, greater sensitivity, and rapid separation when compared to conventional high-performance liquid chromatography (HPLC) methods. Inevitably, UPLC, combined with QTOF-MS, is undoubtedly a suitable system for untargeted metabolomics analysis (Klupczynska et al. 2015; Sreekumar et al. 2009; Wang et al. 2018b; Zhang et al. 2015; Zhou et al. 2018).

Our study showed that ALDH1A1-overexpressed lung adenocarcinoma cells are resistant not only to the molecular-targeted drugs gefitinib and erlotinib, but also to the traditional chemotherapy drug, paclitaxel. We performed metabolic profiling on ALDH1A1-overexpressed lung adenocarcinoma cells using UPLC–QTOF-MS. It is hoped that differential metabolites and metabolic pathways related to ALDH1A1 overexpression will be discovered in HCC827 lung adenocarcinoma. Additionally, more clues for metabolic mechanisms of drug resistance induced by ALDH1A1 may come to light.

2 Materials and methods

2.1 Equipment and reagents

Methanol (MS1922-801, HPLC grade) and water (WS2211-001, HPLC grade) were purchased from TEDIA (Fairfield, USA); acetonitrile (ACN) (1.00030.4000, HPLC grade) was obtained from MERCK (Darmstadt, Germany); formic acid (94318-250 mL-F, MS grade) was purchased from SIGMA (Deisenhofen, Germany); ammonium formate (65929-0025, LCMS grade) was supplied by ROE SCIENTIFIC INC (Newark, USA); phenylalanine-2,3,4,5,6-d5 (D-5466, 99.7 atom % D)

and lysine-4,4,5,5-d4 (D-6689, 98 atom % D) were purchased from CDN isotopes (Canada). Non-small cell lung cancer (NSCLC) therapeutic drugs, including erlotinib (E625000, 500 mg), gefitinib (G304000, 5 g) and paclitaxel (P132500, 250 mg) were obtained from Toronto Research Chemicals, Inc. (North York, Canada). HCC827 cell (ATCC CRL-2868), an NSCLC cell line, was supplied by ATCC (Manassas, VA, USA).

2.2 Cell culture

Cells were cultured using RPMI 1640 medium (Gibco) containing 10% fetal bovine serum (FBS) (GEMINI), 1% GluMax, and 1% penicillin/streptomycin. The cells were maintained at 37 °C under a 5% CO2 atmosphere. HCC827-ALDH1A1 and HCC827-EV cells were cultured in six-well plates at a density of 2.5×10^5 cells/well and harvested when grown to almost 90% confluence. Parallel samples were set up next to experimental samples to determine cell numbers used for data normalization. Adherent cells were washed twice with PBS, quenched in liquid nitrogen for 1 min, and then stored at − 80 °C.

2.3 Construction of ALDH1A1 overexpression vector in HCC827 cell line

A lentivirus for cDNA gene expression was constructed as described previously (Yang et al. 2014). The plasmid, carrying ALDH1A1 coding sequence, was cloned into the lentiviral vector. Then, ALDH1A1 overexpression in HCC827 cells (HCC827-ALDH1A1) was induced using the Tet-On system. Empty vector was used as a control (HCC827-EV). Positive clones were selected for with puromycin after transfection for 72 h. Overexpression of ALDH1A1 was confirmed by real-time PCR and western blotting.

2.4 Cell viability assay

To validate whether or not ALDH1A1-overexpression induces drug resistance in the NSCLC cell line, cell viability assays were performed after treatment with NSCLC therapeutic drugs (erlotinib, gefitinib and paclitaxel). To measure cell viability, CCK-8 assays were performed 72 h after treatment, according to the manufacturer's specifications. At the end of transfection, the cell viability reagent WST-8 was added to each well and incubated for 2 h at 37 °C. Viable cell numbers were estimated by measurement of optical density at 450 nm. The amount of the formazan dye, generated by the activities of dehydrogenases in cells, is directly proportional to the number of living cells.

2.5 Sample preparation

80% methanol aqueous solution containing 100 ng/mL of phenylalanine-2,3,4,5,6-d5 and lysine-4,4,5,5-d4 as internal standard compounds was precooled in a − 80 °C freezer for 10 min, and was then used as a cell lysate. One mL of lysate was added to each well of a six-well plate, and cell samples were scraped into 1.5 mL Eppendorf (EP) tubes, followed by sonication for 30 s, and then centrifuged to remove cellular debris (20,000*g*, 4 °C, 15 min). The supernatants were concentrated in a vacuum centrifugal concentrator for 1 h, then reconstituted with 80 µL of 80% methanol solution for UPLC-MS analysis. Pooled quality control (QC) samples were prepared by mixing 20 µL of each cell sample during extraction procedure.

2.6 UPLC–QTOF-MS method for metabolic profiling

A LC-30AD series Ultra Performance Liquid Chromatography system (Nexera®, Shimadzu, Japan) and a Waters ACQUITY UPLC BEH Amide column (100 × 2.1 mm, 1.7 µm) were used for UPLC–QTOF-MS with a Sciex TripleTOF® 5600 plus mass spectrometer (Sciex, Concord, ON, USA). Data for metabolomics was acquired in both positive (ESI+) and negative (ESI−) modes. The mobile phases in different ionization modes were as follows: (A) 0.1% (v/v) formic acid in acetonitrile and (B) 0.1% (v/v) formic acid in water in ESI+ mode; (A) 10 mM ammonium formate in ACN/H2O (95:5, v/v) and (B) 10 mM ammonium formate in water in ESI− mode. The injection volume was 5 µL and the flow rate was 0.4 mL/min. The following linear gradient was used: 0 min 95% A, 2 min 95% A; 9 min 55% A; 11 min 55% A; 11.2 min 95% A; 15 min 95% A. The column oven was set to 45 °C.

The mass range scanned was m/z 50–1000 in full data storage mode. The drying gas temperature was set at 550 °C (ESI+) and 450 °C (ESI−), the ion spray voltage was 5500 V (ESI+) and − 4500 V (ESI−). Atomization gas pressure, auxiliary heating gas pressure and curtain gas pressure in both ionization modes, were set at 55, 55 and 35 psi, respectively. The instrument was mass calibrated by automatic calibration infusing the Sciex Positive Calibration Solution (part no. 4460131, Sciex, Foster City, CA, USA) for positive mode and Sciex Negative Calibration Solution (part no. 4460134, Sciex, Foster City, CA, USA) for negative mode after every six-sample injections. One QC sample and one blank vial were run after each of the 10 cell samples.

2.7 Statistical analysis

The instrument software MarkerView (version 1.2.1.1, Sciex, USA) was used to perform peak extraction, peak matching, peak alignment and normalization preprocessing

on the acquired data. The main parameters were set as follows: the retention time range was 1–15 min; the retention time and m/z tolerance were 0.1 min and 10 ppm respectively; the response threshold was 100 counts; the isotope peaks were removed. The obtained data set matrix was then imported into the data analysis software SIMCA-P 13.0 (Umetrics, Sweden). After Pareto-scaling (Par transformation), multi-dimensional statistical analysis such as Principal components analysis (PCA) and partial least-squares discrimination analysis (PLS-DA) were performed.

PCA and PLS-DA models were established to visualize metabolic differences among HCC827-ALDH1A1 and HCC827-EV groups. The quality of the models is described by the R^2X (PCA) or R^2Y (PLS-DA) values. To avoid model over-fitting, 999 cross-validations in SIMCA-P 13.0 were performed throughout in order to determine the optimal number of principal components. R^2X, R^2Y and Q^2Y values of the models were nearly 1.0, indicating that these models have good capacity in explaining and predicting variations in the X and Y matrices.

Heat maps were generated with Omicshare platform (Gene Denovo, GuangZhou, China), which is available online at: http://www.omicshare.com/. Error bars in the figures represent SEM. Statistical significance was accepted at *$p < 0.05$; **$p < 0.01$; ***$p < 0.001$;****$p < 0.0001$.

2.8 Identification of metabolic profiles

The different metabolites were determined by the combination of the VIP (variable importance in the projection) value > 1 and and |pcorr| > 0.52 in PLS-DA models and the p values (< 0.05) from two-tailed Student's *t* test on the normalized peak intensities. Fold change was calculated as the average normalized peak intensity ratio between two groups.

The structural identification of differential metabolites was performed by matching the mass spectra with an in-house standard library (Table S2), including accuracy mass, retention time, MS/MS spectra and online databases: Metlin (http://www.metlin.scripps.edu) and HMDB (http://www.hmdb.ca).

2.9 Metabolic pathway analysis

The impact of ALDH1A1 on the metabolic phenotype of HCC827 cells was evaluated based on MetaboAnalyst 4.0 software (Genome Canada, Canada) for pathway analysis, which is available online (http://www.metaboanalyst.ca). The Pathway Analysis module in the tool explores the results interactively and gives detailed instructions and outcomes to obtain a better understanding of the pathways involved in the conditions under study. By uploading the differential metabolites, the built-in pathway library (human) and hypergeometric test for over-representation analysis were employed. A results report was then presented graphically as well as in a detailed table.

3 Results

3.1 ALDH1A1-overexpressed HCC827 cells are resistant to therapeutic drugs

Previous reports have shown a correlation between ALDH and drug resistance (Ajani et al. 2014; Liu et al. 2013). Kanya Honoki et al. found that overexpression of ALDH1 in tumors can confer resistance to chemotherapy (Honoki et al. 2010). ALDH1A1 is one of the 19 ALDH subtypes in humans, and is commonly used to express the activity of tumor stem cell ALDH (Marcato et al. 2011).

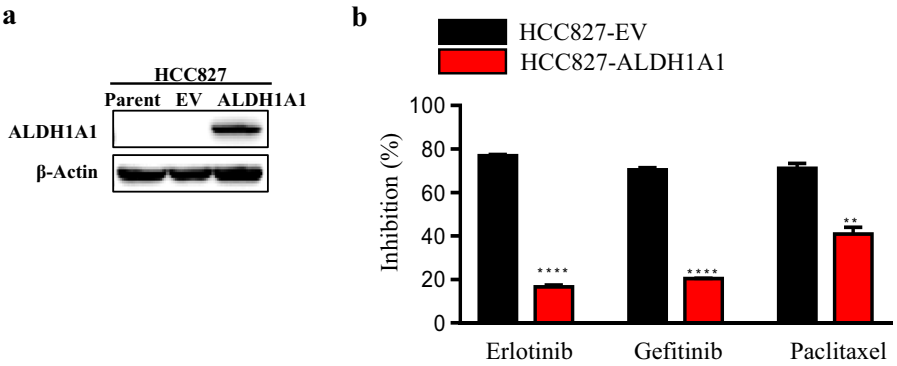

Fig. 1 Drug resistance of ALDH1A1 overexpressed lung adenocarcinoma cells. **a** Western blot analysis of HCC827-parent, HCC827-EV and HCC827ALDH1A1 cells. Blots have been probed with the indicated antibodies. β-actin was used as loading control. **b** The inhibitory rate of HCC827 cells after transfection with ALDH1A1 or control RNA and treatment with erlotinib (1 μM), gefitinib (1 μM) and paclitaxel (100 μM) for 72 h. Statistical analysis was performed using two-tailed Student's *t* test. Error bars in the figures represent SEM. Statistical significance was accepted at *$p < 0.05$; **$p < 0.01$; ***$p < 0.001$; **** $p < 0.0001$

Western blotting analysis revealed that ALDH1A1 overexpression occurred in HCC827-ALDH1A1 cells (Fig. 1a), which indicated that we successfully constructed ALDH1A1-overexpressed cells. Quantitative real-time PCR analysis also demonstrated higher expression levels of ALDH1A1 in HCC827-ALDH1A1 cells (Fig. S2).

To clarify the effect of ALDH1A1 on cell proliferation under drug treatment (erlotinib 1 μM, gefitinib 1 μM and paclitaxel 100 μM), we conducted CCK-8 assays in HCC827-ALDH1A1 and HCC827-EV cells. ALDH1A1 overexpression significantly enhanced the proliferation of HCC827-ALDH1A1 cells, while the proliferation of HCC827-EV cells was remarkably repressed (Fig. 1b). This illustrated that HCC827-ALDH1A1 cells are resistant to erlotinib, gefitinib and paclitaxel. Together, these results suggested that ALDH1A1 was the cellular mediator of drug resistance. ALDH1A1 is one of the principal metabolic enzymes responsible for the oxidation of aldehydes to carboxylic acids, and changes in cellular metabolism accompany classical chemoresistance and tumorigenesis (DeBerardinis and Chandel 2016; Rabold et al. 2017; Sarvi et al. 2018). Hence, alterations in metabolic profiling can specifically reflect the beginning of drug resistance. Metabolic studies may supply potential biomarkers and novel therapeutic strategies to reverse resistance.

3.2 UPLC–QTOF-MS analysis for metabolic profiling

To investigate the contribution of ALDH1A1 to metabolic heterogeneity, a metabolic profiling analysis was performed on HCC827-ALDH1A1 and HCC827-EV cells. The UPLC–QTOF-MS system was able to obtain metabolic profiling for both groups using the total ion chromatogram (TIC). A total of 2088 and 840 features were detected after removing isotope peaks in the positive and negative ion modes respectively. Each feature is composed of exact mass, retention time, and average intensity. From the TICs, there are many different features in the endo-metabolome between the two groups (Fig. 2 and Fig. S3). As shown in Fig. 2, the difference is mainly concentrated in the 4–9 min interval in the positive mode, indicating that more variables may come from this time range. Additionally this difference mainly exists in 3–8 min in the negative mode (Fig. S3).

3.3 Multivariate statistical analysis

For ESI-MS data, 2088 peaks of positive ions and 840 peaks of negative ions from 1 to 15 min of retention time were obtained after data pre-processing. To investigate global metabolic alterations in HCC827-ALDH1A1 and HCC827-EV cells, all observations acquired in both ion modes were integrated and co-analyzed using PCA. PCA, based on cellular metabolites, demonstrated that the two cell lines clustered closely within each group, and separately from each other (Figs. S5a, S6a). QC samples were clustered together,

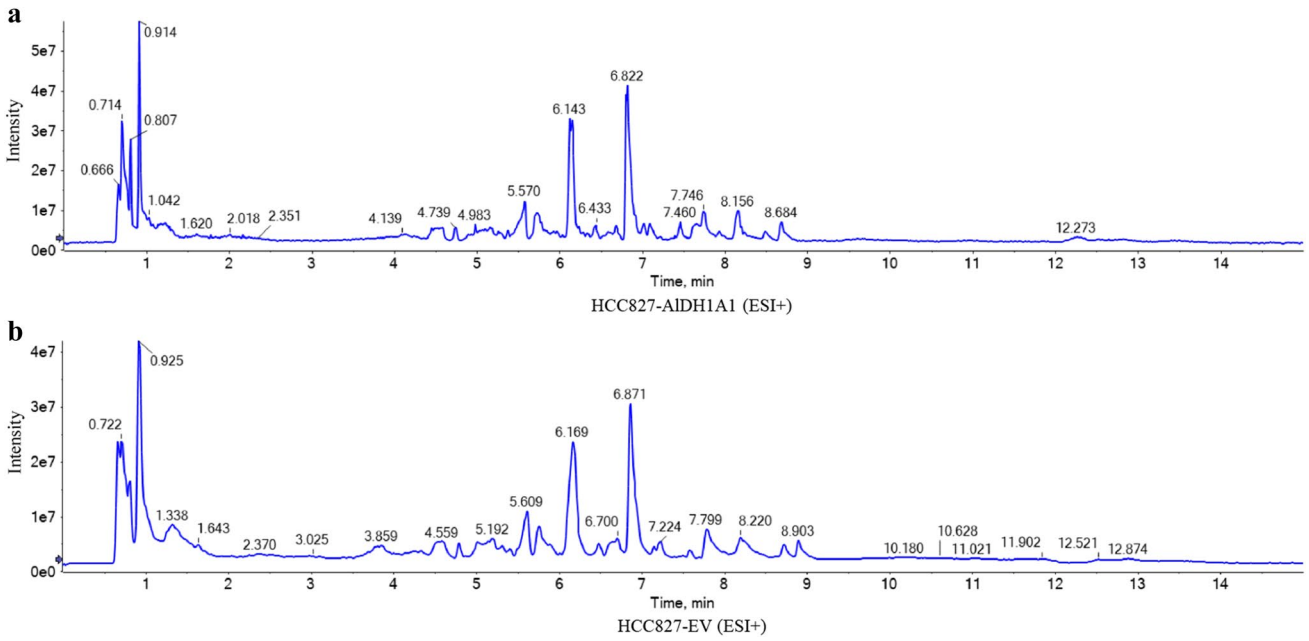

Fig. 2 LC-MS total ion chromatography (TIC) of intracellular metabolites in HCC827-ALDH1A1 and HCC827-EV cells. The UPLC–QTOF-MS system can obtain metabolic profiling of both groups with TIC. **a, b** Detected in the positive (ESI+) ion mode

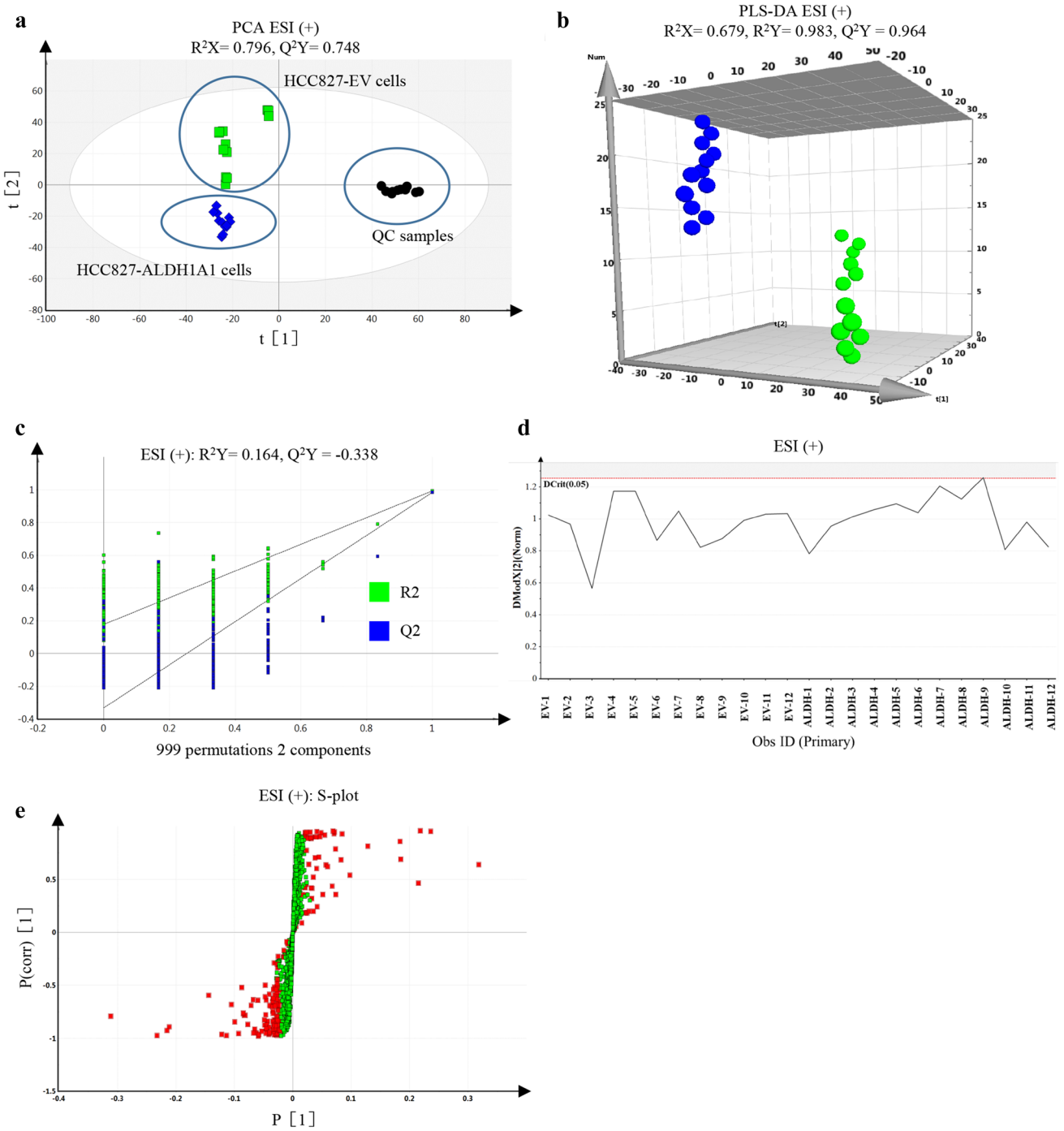

Fig. 3 Multivariate statistical analysis of HCC827-ALDH1A1 and HCC827-EV cells. **a** Score plot for PCA model of HCC827-ALDH1A1 and HCC827-EV cells in ESI+. The black spheres represent quality control samples, the blue diamonds represent HCC827-ALDH1A1 samples, the green squares represent HCC827-EV samples. **b** Score plot for PLS-DA model of HCC827-ALDH1A1 and HCC827-EV cells in ESI+. The blue spheres represent HCC827-ALDH1A1 samples, the green spheres represent HCC827-EV samples. **c** Validation plot of PLS-DA model and 999 RPTs in ESI+. **d** DModX line plot of the model in ESI+. **e** S-plot of the PLS model in ESI+. Each square in the S-plot represents an ion. Ions in red squares are potential biomarkers

indicating good stability and repeatability of the method, which is conducive to the establishment of mathematical models, and to the identification of differential variables (ESI+: $R^2X = 0.796$, $Q^2Y = 0.748$; ESI−: $R^2X = 0.85$, $Q^2Y = 0.836$) (Fig. 3a and Fig. S4a). In loading scatter plots, the further the compounds are from the origin in the loading

plot, the more important they are for the differentiation pattern (Figs. S5b, S6b).

To further explore differences between HCC827-ALDH1A1 and the control group, supervised PLS-DA was applied for stoichiometric analysis. For ESI–MS (+) data, the classification of models and controls resulted in two components with the cross-validated predictive ability $Q^2Y = 0.964$ ($R^2X = 0.679$, $R^2Y = 0.983$) (Fig. 3b). The second model (HCC827-ALDH1A1 vs control in negative ion mode) was produced with an $R^2X = 0.768$, $R^2Y = 0.986$, $Q^2Y = 0.98$ (Fig. S4b). Permutation testing (999 times) showed that the model is not over-fitted (ESI+: $R^2Y = 0.164$, $Q^2Y = -0.338$; ESI−: $R^2Y = 0.232$, $Q^2Y = -0.257$) (Fig. 3c and Fig. S4c). In addition, Distance to Model X (DModX) was applied to test the outliers of the model. In SIMCA, the detection tool for outliers is termed DModX, a short-hand notation for distance to the model in X-space. DModX is based on considering the elements of the residual matrix E and summarizing these row-by-row. A value for DModX can be calculated for each observation. These values can be plotted in a control chart where the maximum tolerable distance (Dcrit) for the dataset is given. Moderate outliers have DModX values larger than Dcrit. When DModX is twice Dcrit, there is some indication of more considerable outliers. The result obtained from the DModX line plot indicated that there were no outliers in our model (Fig. 3d and Fig.S4d). The HCC827-ALDH1A1 group can be separated from EV controls clearly, which reflected the remarkably distinct metabolic status of HCC827-ALDH1A1 and HCC827-EV cells. The S-plot, an easy way to visualize a PLS-DA model of two classes with magnitude (intensity) and reliability, was also used for the selection of biomarkers (Fig. 3e and Fig. S4e). Two vectors, p and p (corr), are combined in S-plot. A high p (corr) means a very high reliability. Variables with a VIP value > 1, p value < 0.05 and p (corr) absolute values > 0.52 were finally considered as different variables. Finally 225 and 118 different variables were found out in positive and negative mode respectively. Multivariate statistical analysis revealed a set of metabolites that discriminated between HCC827-ALDH1A1 and HCC827-EV cells.

3.4 ALDH1A1 distinctly influences metabolic vulnerabilities in NSCLC cells

The selected variables identified by single- and multi-dimensional statistical analysis were matched by matching the mass spectra with an in-house standard library including accuracy mass, retention time and MS/MS spectra. The

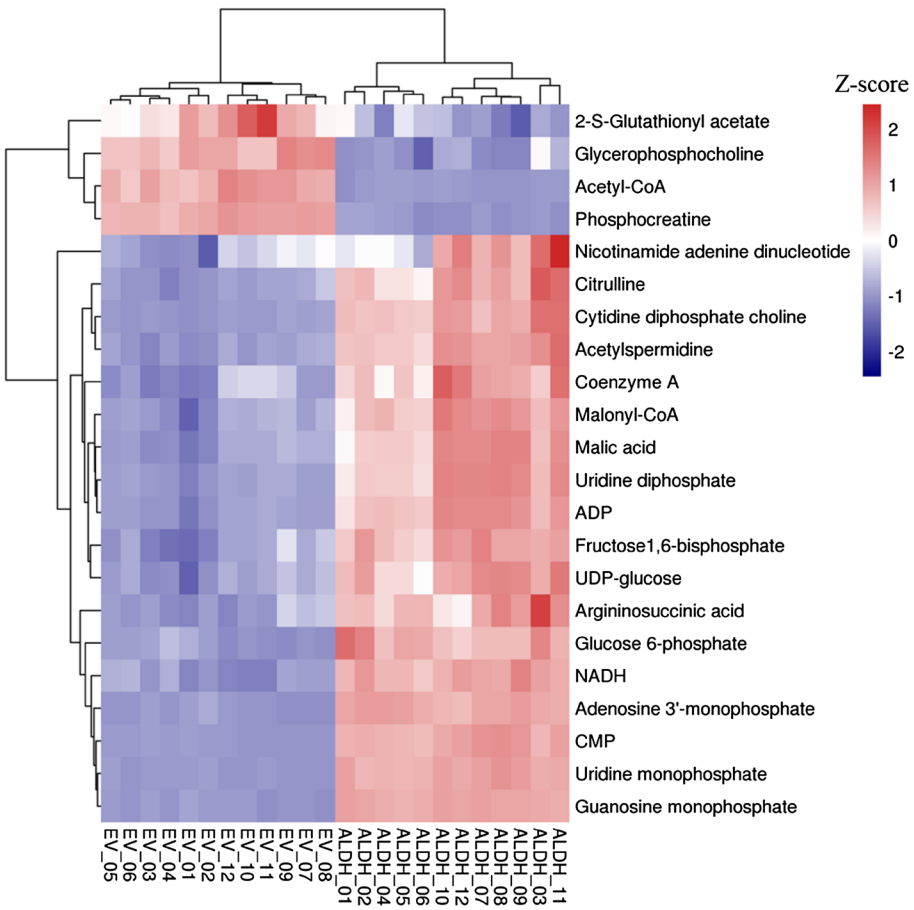

Fig. 4 Heat map of hierarchical clustering using intracellular metabolic data from HCC827-ALDH1A1 and HCC827-EV cells. Each row represents a metabolite and each column represents a sample. Metabolite features whose levels vary significantly ($p < 0.01$) between HCC827-ALDH1A1 and HCC827-EV cells are projected on the heat map and used for sample clustering. The Z-score of each metabolite is plotted over the firebrick–navy color scale. The firebrick color indicates high abundance and navy indicates low abundance

online databases Metlin and HMDB were used to validate fragment information. Finally, 22 potential biomarkers were identified (Table S1). Data are presented as the mean fold differences in HCC827-ALDH1A1 metabolite abundance, compared to the HCC827-EV group. The heat map showed 22 potential biomarkers and unsupervised clustering of samples using metabolic signatures (Fig. 4).

In Table S1 and Fig. 4, 18 metabolites upregulated in HCC827-ALDH1A1 included uridine monophosphate, 5′-CMP, guanosine monophosphate, uridine diphosphate, adenosine 3′-monophosphate and ADP (> 2-fold), representing pyrimidine and purine metabolism; malic acid (3.21-fold) and malonyl-CoA (1.75-fold), representing the tricarboxylic acid cycle (TCA); glucose 6-phosphate, UDP-glucose, fructose1,6-bisphosphate (> 1.37-fold), representing glycolytic metabolism; citrulline (1.34-fold), argininosuccinic acid (1.33-fold), representing the urea cycle, and cytidine diphosphate choline (2.15-fold), representing glycerophospholipid metabolism. Table S1 further identifies the four metabolites downregulated in HCC827-ALDH1A1. These include 2-*S*-glutathionyl acetate (0.82-fold), representing glutathione metabolism, phosphocreatine (0.59-fold), representing the ammonia cycle, and glycerophosphocholine (0.78-fold), representing lipid metabolism. Information regarding metabolite names, retention times, the detected masses (Da), the mass error (ppm), fold change, p values, direction of change, Kyoto Encyclopedia of Genes and Genomes (KEGG), Human Metabolome DataBase (HMDB), and PubChem identifiers for all 22 metabolites is listed in Table S1.

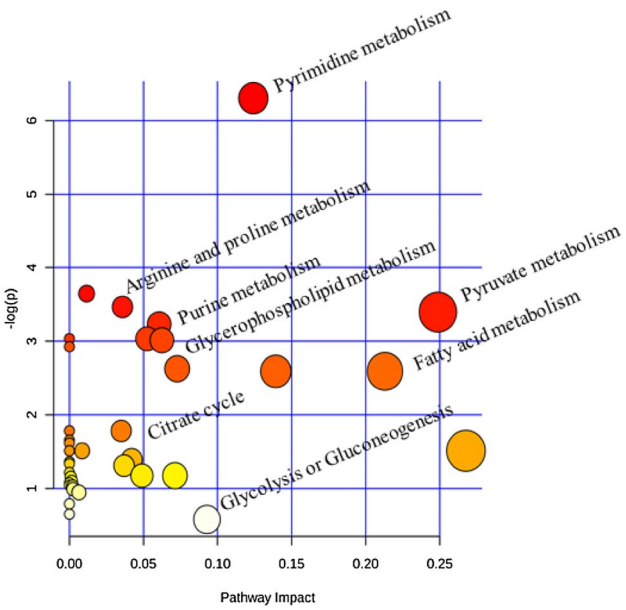

Fig. 5 Analysis of pathway enrichment by differential metabolites in HCC827-ALDH1A1 and HCC827-EV cells. Significantly altered pathways were determined by completing pathway enrichment analysis within MetaboAnalyst 4.0 software. Pathway enrichment, the abscissa pathway impact represents the influencing factor of the path topological analysis, and the ordinate −log(p) represents the p value of the pathway enrichment analysis (negative logarithm). At the same time, the bubble size indicates the influence factor of topological analysis, the bigger the bubble is, the bigger the impact factor is. The color of the bubbles indicates the p value (negative logarithm) of the enrichment analysis. The darker the color, the larger the value of −log(p), the more significant the enrichment

3.5 Pathway enrichment analysis

In this study, the data were input into online MetaboAnalyst 4.0 and metabolic pathways were analyzed to identify which pathways are largely involved in (Fig. 5). Relationships between most of the differential metabolites are shown in Fig. 6, where red-labeled metabolites were elevated in HCC827-ALDH1A1 cells, and green-labeled metabolites were decreased in those cells. Pyrimidine and purine metabolism were enhanced in HCC827-ALDH1A1, reflecting that the biosynthesis of nucleotides was enriched. Nucleotides are essential biomolecules and are the building blocks of nucleic acids within cells. They are also involved in a variety of cellular functions that require energy in the form of the adenosine triphosphate (ATP), guanosine triphosphate, cytidine triphosphate and uridine triphosphate. Several amino acid metabolic pathways were altered, including arginine and proline metabolism. Amino acids are the source of biological macromolecular proteins, including enzymes, transport proteins, and other functional polypeptides. Functional proteins play important cellular roles, including metabolic reactions, DNA replication, and signaling. In addition, reactions related to energy metabolism, such as TCA cycle and glucose metabolism, were also enhanced. Energy is a primary requirement for cancer cell survival, proliferation and migration. The enrichment of these metabolic pathways may reflect cellular energy demands. These metabolic pathways might directly or indirectly reflect the drug resistance capacity of NSCLC cells.

4 Discussion

In our study, ALDH1A1 was indeed associated with tumor cell resistance, with increased expression in tumor cells making tumor cells resistant to therapeutic drugs (Fig. 1). Specific oncogenotypes can produce distinct metabolic changes in certain types of cancer (Boroughs and DeBerardinis 2015; Faubert et al. 2014). Metabolic reprogramming usually occurs in tumor cells because it meets the needs of tumor survival, proliferation and other aspects. These metabolic changes are caused by the activation of tumor cell oncogenes, which can alter the metabolism of tumors

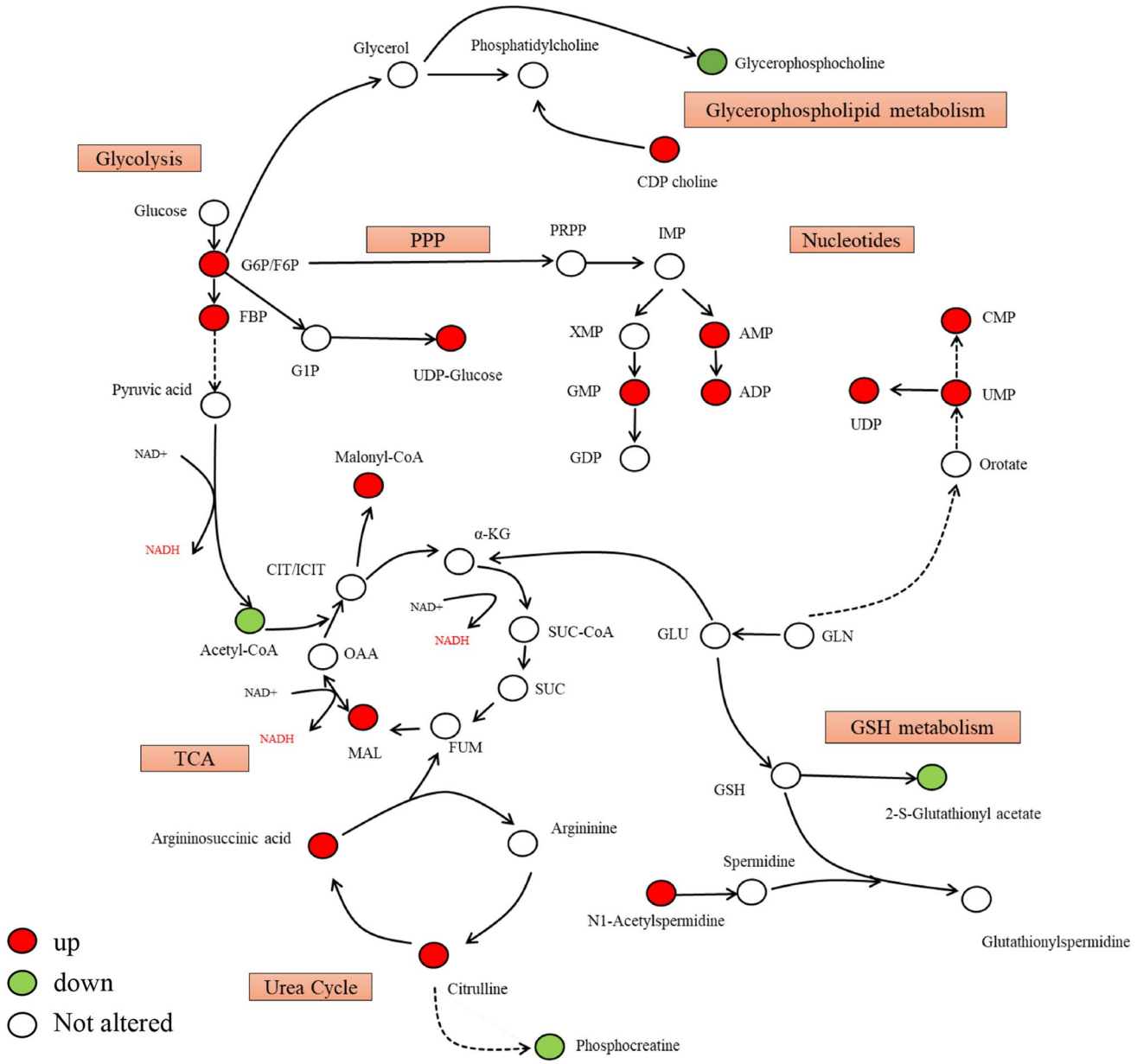

Fig. 6 Schematic overview of metabolic changes in HCC827-ALDH1A1 and HCC827-EV cells. Metabolites marked in red were significantly upregulated in HCC827-ALDH1A1 cells versus HCC827-EV cells. The metabolites marked in green were significantly downregulated in HCC827-ALDH1A1 cells versus HCC827-EV cells

through the coordinated operation of various signaling pathways (Sciacovelli et al. 2014).

In order to adapt to the environment and maintain rapid growth and proliferation, drug-resistant cells generally change their core metabolism. Maiso et al. (2015) found that inhibition of glycolysis can effectively inhibit the proliferation of drug-resistant tumor cells. Kuntz et al. (2017) even suggested that relapse in chronic myeloid leukemia drug resistance is due to metabolic reprogramming of CSCs, which can effectively inhibit the drug-resistant recurrence of leukemia after targeting mitochondrial energy metabolism. In Figs. 2 and 3, we show that the metabolic profile of HCC827-ALDH1A1 cells changed significantly, suggesting that ALDH1A1 can maintain tumor resistance through cellular metabolic reprogramming. ALDH is an enzyme that can catalyze the oxidation of aldehydes to carboxylic acids, and is indeed associated with multiple tumor relapses and poor prognosis (Croker and Allan 2012; Sladek and Landkamer 1985; Storms et al. 1999). Stass et al. found that ALDH-positive lung cancer cells have greater drug resistance, self-renewal ability and tumor formation ability (Jiang et al. 2009). Ginestier revealed that ALDH1A1 is a human breast

tumor and bladder CSC marker and a predictor of poor prognosis (Ginestier et al. 2007; Su et al. 2010). Metabolomics can directly reflect the phenotype of cells by detecting intracellular metabolites and amplifies small changes in gene and protein expression at metabolic levels. However, whereas there are few studies on ALDH overexpressed tumor cell metabolomics, we continue to explore this field and hope to provide new research directions and data for its role in tumor resistance and poor prognosis.

In our study, ALDHA1A1 overexpressed lung adenocarcinoma cells were constructed, and a UPLC–QTOF-MS-based cell metabolic profiling method was established (Fig. 1 and Table S1). We found that the level of metabolites in the glycolytic pathway was up-regulated, suggesting that ALDHA1A1 overexpressing lung adenocarcinoma cells can satisfy the rapid growth of tumor cells or respond to drug stress through the Warburg effect (Fig. 6). The Warburg effect is a typical metabolic feature in tumor cells, which can utilize glucose metabolites to produce important biomacromolecules such as lipids, ribose, and glycerol, so as to provide a nutrient source for tumor proliferation. It has been reported that when targeting glycolysis in breast cancer resistant cells, the Warburg effect can effectively overcome tumor resistance to trastuzumab (Zhao et al. 2011).

As shown in Figs. 4 and 5, we also found changes in the levels of metabolites such as CDP choline and glycerol phosphatidylcholine, indicating that ALDHA1A1 overexpressed lung adenocarcinoma cells do regulate glycerophospholipid metabolism, the source of which is likely to be derived from intermediate metabolites of glycolysis. Bao et al. (2016) proposed that high levels of glycerophospholipid metabolism in malignant melanoma are associated with poor prognosis, suggesting that drug-resistant cells may require a large amount of lipids due to the synthesis of cell membranes and signaling molecules, and thus tumor cells may enhance the metabolism of glycerophospholipids. Meanwhile, the citric acid in the TCA cycle could be converted to propionyl-CoA by the action of ATP citrate lyase and acetyl-coenzyme carboxylase, and then converted to palmitic acid by the action of fatty acid synthase. Our study found that the propionyl-CoA and malic acid content increased significantly, implicating energetic metabolism was enhanced when ALDH1A1 was overexpressed (Fig. 6). In patients with drug-resistant breast and ovarian cancer, previous studies have also found that fatty acid synthase expression is up-regulated and fatty acid metabolism is enhanced (Bauerschlag et al. 2015; Munoz-Pinedo et al. 2012).

Tumors require a large amount of nucleotides as raw materials during the process of malignant proliferation. A class of anti-nucleotide synthetic drugs, including 5-fluorouracil and 6-mercaptopurine, have been used effectively as tumor chemotherapy drugs, thereby indicating that nucleotide metabolism is crucial in tumors. We found that in ALDH overexpressed tumor cells, levels of nucleotide metabolites, such as cytidine monophosphate (CMP), uridine monophosphate (UMP), adenosine monophosphate (AMP), and guanosine monophosphate (GMP) were increased (Fig. 5), indicating that enhanced nucleotide metabolism facilitates the survival and proliferation of drug-resistant cells. Cui Y et al. (2014) found that nuclear factor kappa-light-chain-enhancer of activated B cells 2 (NF-κB2) can regulate 6-phosphate glucose dehydrogenase to promote glucose 6-phosphate into the pentose phosphate pathway (PPP) to enhance nucleotide metabolism in prostate cancer cells. Furthermore, NF-κB2 can promote tumor growth and also enhance drug resistance in tumor cells (Nadiminty et al. 2013). Arginine is an intermediate metabolite in the urea cycle. Citrulline and aspartic acid are synthesized by argininosuccinic acid by argininosuccinate synthetase, and then become fumaric acid and arginine, catalyzed by argininosuccinate lyase, in which fumaric acid is a component of the TCA cycle, which links the urea cycle with energy metabolism. We found that the content of citrulline and argininosuccinic acid increased in HCC827-ALDH1A1 cells, indicating that the urea cycle was in an enhanced state, while the arginine content did not change significantly, probably because arginine was involved in multiple metabolic pathways, such as the biosynthesis of creatine and polyamines, and anabolism of nucleotides, proline and glutamate.

5 Conclusion

In summary, we established UPLC–QTOF-MS-based intracellular metabolic profiling analysis of HCC827-ALDH1A1 cells and found that ALDH1A1, a major metabolic enzyme, enables tumors to be resistant to therapeutic drugs. The metabolic profile of HCC827-ALDH1A1 cells was altered, and most metabolites, such as glucose-6-phosphate, fructose 1,6-diphosphate, propionyl-CoA, malic acid, malic acid, phosphatidylcholine, glycerol phosphatidylcholine, GMP, citrulline and arginine succinic acid increased, involving metabolic pathways such as glycolysis, the TCA cycle, glycerophospholipid metabolism, nucleotide metabolism, and the urea cycle. Enhanced metabolic phenotypes of energy metabolism and anabolism induced by ALDH1A1 promote drug resistance of tumor cells to therapeutic drugs. Among them, differential metabolites are largely involved in nucleotide metabolic pathways, and ALDH may affect tumor resistance through such pathways (Fig. 6). Our study provides a metabolic dissection of HCC827-ALDH1A1 cells, offering insights into drug resistance mechanisms, and proposes related differential metabolic pathways, which provides clues for drug-resistant tumor molecular mechanisms and drug targets.

Acknowledgements This work was supported by the Natural Science Foundation of China (Grant Nos. 81872822, 81573018), the Shanghai Municipal Science Foundation (Grant Nos. 14YZ032, 2013-52), and the Scientific Research Foundation of the State Education Ministry for Returned Overseas Chinese Scholars (Grant No. 2013/45).

Author contributions Yang Wang, Cong-Hui Wang, Yu-Fei Zhang, Liang Zhu, Hui-Min Lei, Ya-Bin Tang conceived and planned the experiments. Yang Wang carried out the experiments, and lead in writing the manuscript. Cong-Hui Wang contributed to sample preparation. Yu-Fei Zhang contributed to the interpretation of results. Liang Zhu verified the analytical methods. Liang Zhu, Hui-Min Lei and Ya-Bin Tang supervised the findings of this work. All authors provided critical feedback and helped shape the research, analysis and manuscript.

Compliance with ethical standards

Conflicts of interest The authors declare that they have no conflicts of interests in relation to the work described here.

Research involving human and/or animals participants This work did not involve any human and/or animal participants.

Data availability The metabolomics and metadata reported in this paper are available via MetaboLights (https://www.ebi.ac.uk/metabolights/) study identifier MTBLS830.

References

Ajani, J. A., Wang, X., Song, S., Suzuki, A., Taketa, T., Sudo, K., et al. (2014). ALDH-1 expression levels predict response or resistance to preoperative chemoradiation in resectable esophageal cancer patients. *Molecular Oncology, 8,* 142–149.

Bao, J., Liu, F., Zhang, C., Wang, K., Jia, X., Wang, X., et al. (2016). Anti-melanoma activity of Forsythiae Fructus aqueous extract in mice involves regulation of glycerophospholipid metabolisms by UPLC/Q-TOF MS-based metabolomics study. *Scientific Reports, 6,* 39415.

Bauerschlag, D. O., Maass, N., Leonhardt, P., Verburg, F. A., Pecks, U., Zeppernick, F., et al. (2015). Fatty acid synthase overexpression: Target for therapy and reversal of chemoresistance in ovarian cancer. *Journal of Translational Medicine, 13,* 146.

Boroughs, L. K., & Deberardinis, R. J. (2015). Metabolic pathways promoting cancer cell survival and growth. *Nature Cell Biology, 17,* 351–359.

Bozorgi, A., Khazaei, M., & Khazaei, M. R. (2015). New findings on breast cancer stem cells: A review. *Journal of Breast Cancer, 18,* 303–312.

Croker, A. K., & Allan, A. L. (2012). Inhibition of aldehyde dehydrogenase (ALDH) activity reduces chemotherapy and radiation resistance of stem-like ALDHhiCD44(+) human breast cancer cells. *Breast Cancer Research and Treatment, 133,* 75–87.

Cui, Y., Nadiminty, N., Liu, C., Lou, W., Schwartz, C. T., & Gao, A. C. (2014). Upregulation of glucose metabolism by NF-kappaB2/p52 mediates enzalutamide resistance in castration-resistant prostate cancer cells. *Endocrine-Related Cancer, 21,* 435–442.

Deberardinis, R. J., & Chandel, N. S. (2016). Fundamentals of cancer metabolism. *Science Advances, 2,* e1600200.

Domingues, D., Turner, A., Silva, M. D., Marques, D. S., Mellidez, J. C., Wannesson, L., et al. (2014). Immunotherapy and lung cancer: Current developments and novel targeted therapies. *Immunotherapy, 6,* 1221–1235.

Faubert, B., Vincent, E. E., Griss, T., Samborska, B., Izreig, S., Svensson, R. U., et al. (2014). Loss of the tumor suppressor LKB1 promotes metabolic reprogramming of cancer cells via HIF-1alpha. *Proceedings of the National Academy of Sciences of the USA, 111,* 2554–2559.

Ginestier, C., Hur, M. H., Charafe-Jauffret, E., Monville, F., Dutcher, J., Brown, M., et al. (2007). ALDH1 is a marker of normal and malignant human mammary stem cells and a predictor of poor clinical outcome. *Cell Stem Cell, 1,* 555–567.

Honoki, K., Fujii, H., Kubo, A., Kido, A., Mori, T., Tanaka, Y., et al. (2010). Possible involvement of stem-like populations with elevated ALDH1 in sarcomas for chemotherapeutic drug resistance. *Oncology Reports, 24,* 501–505.

Huang, C. P., Tsai, M. F., Chang, T. H., Tang, W. C., Chen, S. Y., Lai, H. H., et al. (2013). ALDH-positive lung cancer stem cells confer resistance to epidermal growth factor receptor tyrosine kinase inhibitors. *Cancer Letters, 328,* 144–151.

Januchowski, R., Wojtowicz, K., & Zabel, M. (2013). The role of aldehyde dehydrogenase (ALDH) in cancer drug resistance. *Biomedicine & Pharmacotherapy, 67,* 669–680.

Januchowski, R., Wojtowicz, K., Sterzyska, K., Sosiska, P., Andrzejewska, M., Zawierucha, P., et al. (2016). Inhibition of ALDH1A1 activity decreases expression of drug transporters and reduces chemotherapy resistance in ovarian cancer cell lines. *International Journal of Biochemistry & Cell Biology, 78,* 248–259.

Jiang, F., Qiu, Q., Khanna, A., Todd, N. W., Deepak, J., Xing, L., et al. (2009). Aldehyde dehydrogenase 1 is a tumor stem cell-associated marker in lung cancer. *Molecular Cancer Research, 7,* 330–338.

Klupczynska, A., Derezinski, P., & Kokot, Z. J. (2015). Metabolomics in medical sciences—trends, challenges and perspectives. *Acta Poloniae Pharmaceutica, 72,* 629–641.

Kobayashi, S., Boggon, T. J., Dayaram, T., Janne, P. A., Kocher, O., Meyerson, M., et al. (2005). EGFR mutation and resistance of non-small-cell lung cancer to gefitinib. *New England Journal of Medicine, 352,* 786–792.

Kuntz, E. M., Baquero, P., Michie, A. M., Dunn, K., Tardito, S., Holyoake, T. L., et al. (2017). Targeting mitochondrial oxidative phosphorylation eradicates therapy-resistant chronic myeloid leukemia stem cells. *Nature Medicine, 23,* 1234–1240.

Lassen, N., Bateman, J. B., Estey, T., Kuszak, J. R., Nees, D. W., Piatigorsky, J., et al. (2007). Multiple and additive functions of ALDH3A1 and ALDH1A1: Cataract phenotype and ocular oxidative damage in Aldh3a1(−/−)/Aldh1a1(−/−) knock-out mice. *Journal of Biological Chemistry, 282,* 25668–25676.

Liu, J., Xiao, Z., Wong, S. K., Tin, V. P., Ho, K. Y., Wang, J., et al. (2013). Lung cancer tumorigenicity and drug resistance are maintained through ALDH(hi)CD44(hi) tumor initiating cells. *Oncotarget, 4,* 1698–1711.

Luo, Y., Dallaglio, K., Chen, Y., Robinson, W. A., Robinson, S. E., McCarter, M. D., et al. (2012). ALDH1A isozymes are markers of human melanoma stem cells and potential therapeutic targets. *Stem Cells, 30,* 2100–2113.

Magni, M., Shammah, S., Schiro, R., Mellado, W., Dalla-Favera, R., & Gianni, A. M. (1996). Induction of cyclophosphamide-resistance by aldehyde-dehydrogenase gene transfer. *Blood, 87,* 1097–1103.

Maiso, P., Huynh, D., Moschetta, M., Sacco, A., Aljawai, Y., Mishima, Y., et al. (2015). Metabolic signature identifies novel targets for drug resistance in multiple myeloma. *Cancer Research, 75,* 2071–2082.

Manzer, R., Qamar, L., Estey, T., Pappa, A., Petersen, D. R., & Vasiliou, V. (2003). Molecular cloning and baculovirus expression of the rabbit corneal aldehyde dehydrogenase (ALDH1A1) cDNA. *DNA and Cell Biology, 22,* 329–338.

Marcato, P., Dean, C. A., Giacomantonio, C. A., & Lee, P. W. (2011). Aldehyde dehydrogenase: Its role as a cancer stem cell marker comes down to the specific isoform. *Cell Cycle, 10,* 1378–1384.

Munoz-Pinedo, C., el Mjiyad, N., & Ricci, J. E. (2012). Cancer metabolism: Current perspectives and future directions. *Cell Death & Differentiation, 3,* e248.

Nadiminty, N., Tummala, R., Liu, C., Yang, J., Lou, W., Evans, C. P., et al. (2013). NF-kappaB2/p52 induces resistance to enzalutamide in prostate cancer: Role of androgen receptor and its variants. *Molecular Cancer Therapeutics, 12,* 1629–1637.

Nicholson, J. K., & Lindon, J. C. (2008). Systems biology: Metabonomics. *Nature, 455,* 1054–1056.

Prabavathy, D., Swarnalatha, Y., & Ramadoss, N. (2018). Lung cancer stem cells-origin, characteristics and therapy. *Stem Cell Investig, 5,* 6.

Rabold, K., Netea, M. G., Adema, G. J., & Netea-Maier, R. T. (2017). Cellular metabolism of tumor-associated macrophages—functional impact and consequences. *FEBS Letters, 591,* 3022–3041.

Roengvoraphoj, M., Tsongalis, G. J., Dragnev, K. H., & Rigas, J. R. (2013). Epidermal growth factor receptor tyrosine kinase inhibitors as initial therapy for non-small cell lung cancer: focus on epidermal growth factor receptor mutation testing and mutation-positive patients. *Cancer Treatment Reviews, 39,* 839–850.

Sarvi, S., Crispin, R., Lu, Y., Zeng, L., Hurley, T. D., Houston, D. R., et al. (2018). ALDH1 Bio-activates Nifuroxazide to eradicate ALDH(High) melanoma-initiating cells. *Cell Chemical Biology, 25,* 1456.

Sciacovelli, M., Gaude, E., Hilvo, M., & Frezza, C. (2014). The metabolic alterations of cancer cells. *Methods in Enzymology, 542,* 1–23.

Siegel, R., Ma, J., Zou, Z., & Jemal, A. (2014). Cancer statistics, 2014. *CA: A Cancer Journal for Clinicians, 64,* 9–29.

Sladek, N. E., & Landkamer, G. J. (1985). Restoration of sensitivity to oxazaphosphorines by inhibitors of aldehyde dehydrogenase activity in cultured oxazaphosphorine-resistant L1210 and cross-linking agent-resistant P388 cell lines. *Cancer Research, 45,* 1549–1555.

Sreekumar, A., Poisson, L. M., Rajendiran, T. M., Khan, A. P., Cao, Q., Yu, J., et al. (2009). Metabolomic profiles delineate potential role for sarcosine in prostate cancer progression. *Nature, 457,* 910–914.

Storms, R. W., Trujillo, A. P., Springer, J. B., Shah, L., Colvin, O. M., Ludeman, S. M., et al. (1999). Isolation of primitive human hematopoietic progenitors on the basis of aldehyde dehydrogenase activity. *Proceedings of the National Academy of Sciences of the USA, 96,* 9118–9123.

Su, Y., Qiu, Q., Zhang, X., Jiang, Z., Leng, Q., Liu, Z., et al. (2010). Aldehyde dehydrogenase 1 A1-positive cell population is enriched in tumor-initiating cells and associated with progression of bladder cancer. *Cancer Epidemiology, Biomarkers and Prevention, 19,* 327–337.

Sundar, R., Soong, R., Cho, B. C., Brahmer, J. R., & Soo, R. A. (2014). Immunotherapy in the treatment of non-small cell lung cancer. *Lung Cancer, 85,* 101–109.

Tanei, T., Morimoto, K., Shimazu, K., Kim, S. J., Tanji, Y., Taguchi, T., et al. (2009). Association of breast cancer stem cells identified by aldehyde dehydrogenase 1 expression with resistance to sequential Paclitaxel and epirubicin-based chemotherapy for breast cancers. *Clinical Cancer Research, 15,* 4234–4241.

Ueshima, Y., Matsuda, Y., Tsutsumi, M., & Takada, A. (1993). Role of the aldehyde dehydrogenase-1 isozyme in the metabolism of acetaldehyde. *Alcohol and Alcoholism. Supplement, 1B,* 15–19.

Vasiliou, V., Pappa, A., & Petersen, D. R. (2000). Role of aldehyde dehydrogenases in endogenous and xenobiotic metabolism. *Chemico-Biological Interactions, 129,* 1–19.

Vasiliou, V., Pappa, A., & Estey, T. (2004). Role of human aldehyde dehydrogenases in endobiotic and xenobiotic metabolism. *Drug Metabolism Reviews, 36,* 279–299.

Wang, N. N., Wang, L. H., Li, Y., Fu, S. Y., Xue, X., Jia, L. N., et al. (2018a). Targeting ALDH2 with disulfiram/copper reverses the resistance of cancer cells to microtubule inhibitors. *Experimental Cell Research, 362,* 72–82.

Wang, W., Zhao, L., He, Z., Wu, N., Li, Q., Qiu, X., et al. (2018b). Metabolomics-based evidence of the hypoglycemic effect of Ge-Gen-Jiao-Tai-Wan in type 2 diabetic rats via UHPLC-QTOF/MS analysis. *Journal of Ethnopharmacology, 219,* 299–318.

Wettersten, H. I., & Weiss, R. H. (2013). Applications of metabolomics for kidney disease research: From biomarkers to therapeutic targets. *Organogenesis, 9,* 11–18.

Yang, Y., Zhou, W., Xia, J., Gu, Z., Wendlandt, E., Zhan, X., et al. (2014). NEK2 mediates ALDH1A1-dependent drug resistance in multiple myeloma. *Oncotarget, 5,* 11986–11997.

Zhang, Z., He, L., Lu, L., Liu, Y., Dong, G., Miao, J., et al. (2015). Characterization and quantification of the chemical compositions of Scutellariae Barbatae herba and differentiation from its substitute by combining UHPLC-PDA-QTOF-MS/MS with UHPLC-MS/MS. *Journal of Pharmaceutical and Biomedical Analysis, 109,* 62–66.

Zhao, Y., Liu, H., Liu, Z., Ding, Y., Ledoux, S. P., Wilson, G. L., et al. (2011). Overcoming trastuzumab resistance in breast cancer by targeting dysregulated glucose metabolism. *Cancer Research, 71,* 4585–4597.

Zhou, Y., Meng, Z., Gan, H., Zheng, Y., Zhu, X., Wu, Z., et al. (2018). Time-course investigation of small molecule metabolites in MAP-stored red blood cells using UPLC–QTOF-MS. *Molecules, 23,* E923.